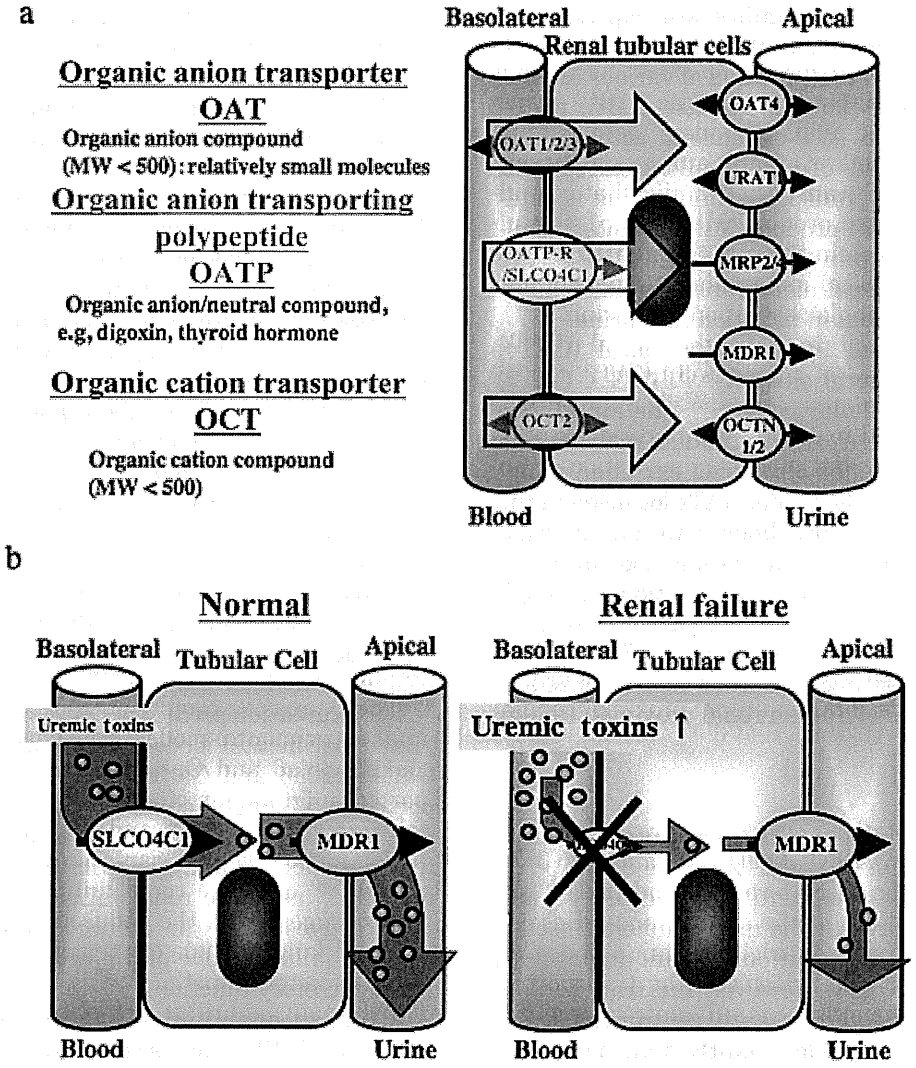

Figure 1. The molecular transporting system of the renal proximal tubular cell. (a) The molecular process of transporting membrane proteins in human proximal tubular cells. The expression patterns are those of OAT(OAT1, OAT2, OAT3), OATP(SLCO4C1) at the basolateral side, and OAT(OAT4, URAT1), and ABC transporters (MDR1, MRP2, MRP4) at the apical side. (b) SLCO4C1 (basolateral) and MDR1 (apical) expression levels in normal and impaired renal tubular cells. In normal kidney, basolateral SLCO4C1 and apical MDR1 work in concert to excrete drugs and uremic toxins from blood into urine. In renal failure states, the expression level of basolateral SLCO4C1, but not MDR1, is downregulated and renal excretory functions decrease.

(i.e., renal slice).[56] Recently, an *in vivo* study of Oat3-konckout mice showed that although renal secretion of PAH is not changed, penicillin G and estrone-3-sulfate plasma clearance were reduced.[57] Another study reported impaired clearance of methotrexate (MTX) in Oat3-knockout mice.[58] However, although the renal clearance of a prototypical anionic compound, for example, PAH, or established substrates transported by OATs such as penicillin G, estrone-3-sulfate, and MTX are significantly changed in Oat-knockout animals, so far there has yet been no report of plasma concentration or renal clearance changes in representative uremic toxins such as IS, CMPF, IAA, and HA. The redundancy of Oat expression (both Oat1 and Oat3 expressed at basolateral side of proximal tubules) and some overlap of the substrate specificity (IS is transpoted not only by Oat1 but also by Oat3) might abrogate the effect of a single-Oat gene deletion. Moreover, as several Oatps are also expressed in mice kidney and some of them are distributed in proximal tubules[23,59] (Table 1), the possible compensated renal elimination of uremic toxins by these Oatps

Table 1. Organic Anion Transporter Polypeptides

Protein Name	Gene Symbol	Novel Protein Name	Novel gene Symbol	Expression
Human OATP				
PGT	*SLC21A2*	OATP2A1	*SLCO2A1*	Widely
OATP-A	*SLC21A3*	OATP1A2	*SLCO1A2*	Brain
LST-1/OATP-C/OATP2	*SLC21A6*	OATP1B1	*SLCO1B1*	Liver only
LST-2/OATP8	*SLC21A8*	OATP1B3	*SLCO1B3*	Liver only
OATP-B/MOAT1	*SLC21A9*	OATP2B1	*SLCO2B1*	Widely
OATP-D	*SLC21A11*	OATP3A1	*SLCO3A1*	Widely
OATP-E	*SLC21A12*	OATP4A1	*SLCO4A1*	Widely
OATP-F	*SLC21A14*	OATP1C1	*SLCO1C1*	Brain, testis
OATP-J/OATP-RP4	*SLC21A15*	OATP5A1	*SLCO5A1*	Breast
GST/OATP-1	*SLC21A19*	OATP6A1	*SLCO6A1*	Tesits
OATP-R	*SLC21A20*	OATP4C1	*SLCO4C1*	Kidney
Rat oatp				
oatp1	*slc2la1*	Oatp1a1	*Slco1a1*	Kiver, kidney
rPGT	*slc2la2*	Oatp2a1	*Slco2a1*	Widely
OAT-K1 OAT-K2	*slc2la4*	Oatp1a3-v1 Oatp1a3-v2	*Slco1a3*	Kidney
oatp2	*slc2la5*	Oatp1a4	*Slco1a4*	Retina, liver, brain
oatp3	*slc2la7*	Oatp1a5	*Slco1a5*	Retina, brain, liver, kidney
oatp4/risz-1	*slc2la9*	Oatp1b2	*Slco1b2*	Liver only
moat1/oatp-B	*slc2la10*	Oatp2b1	*Slco2b1*	Widely
oatp-D	*slc2la11*	Oatp3a1	*Slco5a1*	Widely
oatp-E	*slc2la12*	Oatp4a1	*Slco4a1*	Widely
oatp5	*slc2la13*	Oatp1a6	*Slco1a6*	Kidney
oatp14	*slc2la14*	Oatp1c1	*Slco1c1*	Brain
rGST-1/oatp16	*slc2la16*	Oatp6b1	*Slco6b1*	Tesits
rGST-2/oatp18	*slc2la18*	Oatp6c1	*Slco6c1*	Tesits
oatp-R	*slc2la20*	Oatp4c1	*Slco4c1*	Kidney

Nomenclature of the organic anion transporter polypeptide family.

cannot be excluded. To clarify the contribution of OATs to the renal excretion of various uremic toxins, further experiments (i.e. double knockout or conditional knockout of Oat1 and Oat3) should be necessary.

OATP Family

Organic anion transporting polypeptide was first isolated as a transporting membrane molecule in the liver, which uptakes bile acids from blood into hepatocytes.[18] So far, 11 human clones and 14 rat clones of OATPs that form the OATP/SLC22/SLCO gene family have been identified.[59] The expression of OATPs is distributed throughout various organs such as the central nervous system, endocrine system (thyroid, pituitary), placenta, reproductive organs (testis, ovary), liver, kidney, and intestine (Table 1). The OATP family is involved in the membrane transport of bile acids, conjugated steroids, thyroid hormone, eicosanoids, peptides, cardiac glycosides (digoxin, digitoxin, ouabain), and numerous drugs.[18,60] OATPs are crucial transporting proteins that regulate the uptake, excretion, and metabolism of various hormones and metabolites. OATPs also determine the drug availability of organs, their elimination, and the pharmacokinetics.[18,59,60]

SLCO4C1, OATP in Kidney

In the kidney, various water-soluble and protein-binding compounds are mainly excreted from blood through renal tubular cells. Several ABC transporters, MRP2, MRP4, and MDR1, are reported to be expressed in the apical membrane of proximal tubular cells and are thought to mediate the tubular secretion of renal-excreted drugs such as digoxin, MTX, and irinotecan.[24–26,29] On the contrary, such drugs have to transverse the basolateral membrane of tubular cells and need membrane transporting proteins. OATPs have thus been regarded as a first step molecule in the transport of digoxin and various compounds into the urine.

We have recently identified a kidney-specific OATP, human SLCO4C1/OATP4C1/OATP-R, and its rat homologue Slco4c1/Oatp4c1/oatp-R.[2] SLCO4C1 is the only OATP expressed in human kidney and is localized at the basolateral membrane of proximal tubular cells. SLCO4C1 transports thyroid hormone, digoxin, an endogenous digoxin-like compound (ouabain), and MTX.[2,7] In a rat renal failure model, renal tubular basolateral rat Slco4c1 expression was decreased.[2] On the contrary, the expression level of MDR1, a member of the ABC transporter family that mediates the tubular secretion of digoxin at the apical membrane of proximal tubular cells, was not changed[24] (Fig. 1b). This reduction of SLCO4C1 in the proximal tubules

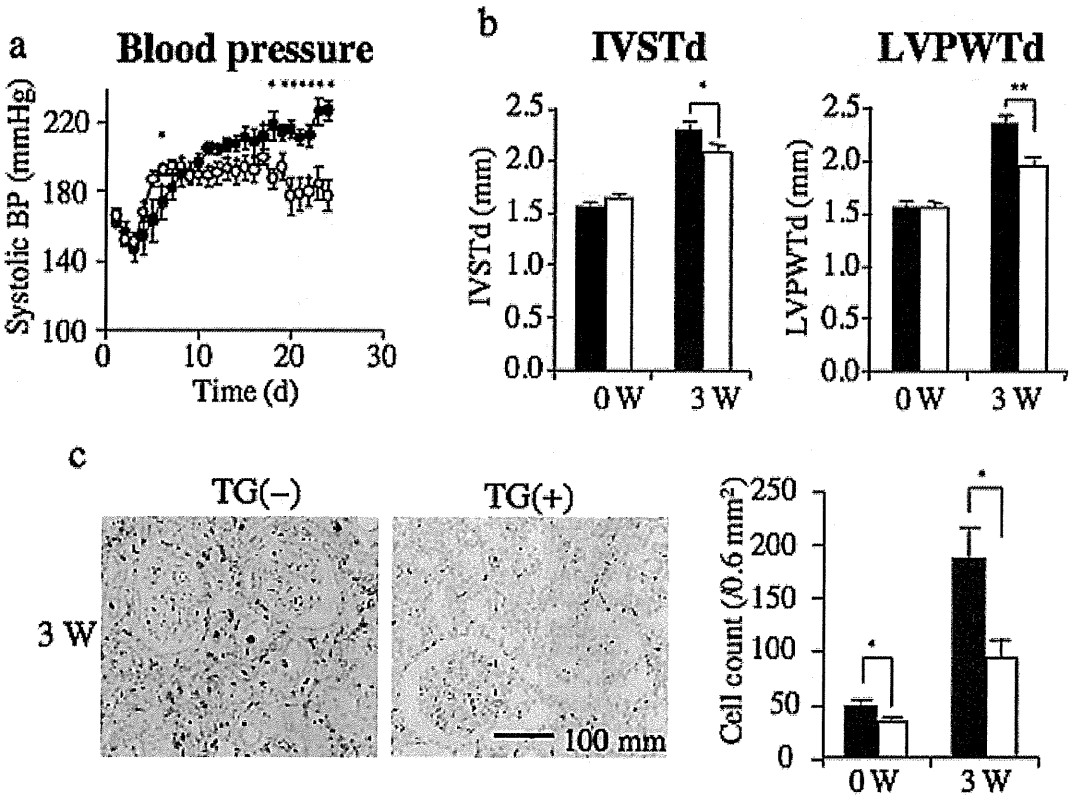

Figure 2. Hypertension, cardiomegaly, and renal inflammation are ameliorated in 5/6-nephrectomized (Nx) human SLCO4C1-proximal tubular cell-specific overexpressing transgenic (TG+) rats compared with TG(−) Nx littermates. (a) Blood pressure TG(−) Nx rats(filled circle) and TG(+) Nx rats(open circle). $^{*}p < 0.05$ versus TG(−) Nx rats. (b) Interventricular septum thickness during diastole (IVSTd) and left ventricular posterior wall thickness during diastole (LVPWTd) were measured by echocardiogram before and 3 weeks after 5/6 nephrectomy. TG(−) Nx rats (filled bar) and TG(+) Nx rats (open bar). $^{*}p < 0.05$, $^{**}p < 0.01$. (c) CD68 staining in the rat kidney before and 3 weeks after 5/6 nephrectomy. CD68-positive cell number counts were performed before and 3 weeks after 5/6 nephrectomy. $^{*}p < 0.05$ compared with TG(−) rat.

may be one of the mechanisms of the impaired urinary excretion of digoxin and drugs in renal failure[2,7] (Fig. 1b). Furthermore, in human, SLCO4C1 is the only OATP in the kidney, whereas several oatps exist at the basolateral and apical membrane of the proximal tubules in rodent kidney[2,7,23,30,60] (Table 1). In rat kidney, Oatp1a1/Slco1a1/oatp1, Oatp1a3-v1,Oatp1a3-v2/Slco1a3/OAT-K1,OAT-K2, Oatp1a7/Slco1a7/oatp3, Oatp1a6/Slco1a6/oatp5, and Oatp4c1/Slco4c1/oatp-R are expressed[23,59] (Table 1). At least, Oatp1a1, Oatp1a3-v1, and Oatp1a3-v2 are reported to be localized on the apical membrane of rat proximal tubules, whereas Oatp4c1 is localized on the basolateral membrane of rat proximal tubules.[23]

However, except for Oatp4c1/Slco4c1, so far no human ortholog of other rodent Oatps have yet been identified[23,59] (Table 1). This species diversity of the OATP family subtypes and their multiple locations in the proximal tubules make it difficult to extrapolate from experimental studies in rodents to human. The redundancy of multiple clones expression in rat kidney and some overlapping transporting properties (i.e., some organic compounds such as thyroid hormones, statins, and conjugated steroids are transported both by Oatp1a1 and Oatp1a7) make it difficult to investigate the contributions of those Oatps within the proximal tubules cells or whole kidney excretion.[18,59,60] To overcome these issues, we generated a transgenic (TG) rat harboring human SLCO4C1 in rat kidney and clarified the physiological and pathophysiological roles of human SLCO4C1.[7]

When the renal mass was reduced by 5/6 nephrectomy (Nx), the BP was significantly decreased in SLCO4C1-transgenic [TG(+)] rat compared with TG(−) littermates (Fig. 2a). In 5/6 nephrectomized SLCO4C1-transgenic [TG(+)Nx] rats, cardiac hypertrophy was also significantly reduced[7] (Fig. 2b).

In CKD patients, renal inflammation is also a risk factor for renal damage, morbidity, and mortality.[61] Immunohistochemically, mononuclear cell infiltration

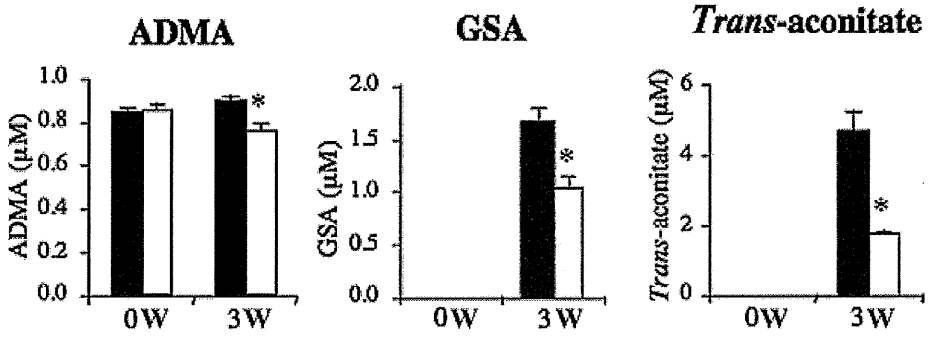

Figure 3. Metabolomic analysis of uremic toxins in rats with CRF. Metabolome analysis and characterization of uremic toxins. The plasma concentration of ADMA, GSA, and *trans*-aconitate before and 3 weeks after 5/6 nephrectomy. TG(−) Nx rats (filled bar) and TG(+) Nx rats(open bar). $^*p < 0.05$.

was strongly detected in TG(−)Nx rat kidneys by the macrophage marker, CD68. On the contrary, TG(+)Nx kidneys demonstrated less infiltration of macrophages (Fig. 2c). These data indicate that the expression of human SLCO4C1 in rat kidneys ameliorated not only the hypertension but also the inflammation in renal failure.

Metabolomic Analysis of Kidney-Specific Human SLCO4C1-TG Rat

A vicious cycle of progressive chronic renal damage occurs in patients with CKD, but there has been no specific therapeutic strategy for renal disease.

The accumulation of toxic uremic solutes, so called "uremic toxins," promotes renal damage, the progression of atherosclerosis, and evokes hypertension and the deterioration of cardiomyopathy (uremic cardiomyopathy) and other CVDs.[12,40] The mortality of patients with CKD, especially end-stage renal disease (ESRD) or those undergoing HD therapy, is very high.

Some of the causes of the poor prognosis and outcomes are derived from the malignant cycle of renal damage and the accumulation of uremic toxins.

Our assumption is that a method to reduce the serum level of uremic toxins and prevent their accumulation in organs could be a beneficial and specific therapeutic modality for CKD that would alleviate the progressive renal damage and reduce the mortality and morbidity of patients with CKD.[7–17] AST-120 is an oral sorbent that absorbs indole in the intestine and reduces the serum IS. AST-120 is administered in CKD patients and ameliorates the progression of CKD,[62] but the removal of uremic toxins is restricted mainly to IS,[63] whereas the accumulation of other harmful uremic toxins is thought to promote renal damage.

Hemodialysis also partially reduces some uremic toxins in patients with CRF, but the reduction of such toxins is transient and followed by an elevation to the previous level by the next HD, whereas other uremic solutes that are not effectively removed by HD still exist aggravating renal damage and CVDs in CRF patients.

Recently, we revealed that many uremic toxins accumulate in renal failure using capillary electrophoresis–mass spectrometry (CE–MS),[64] and that the kidney-specific OAT SLCO4C1 was involved in the excretion of uremic toxins resulting in reductions of the blood pressure and renal inflammation.[7,8] With the progression of CKD, various uremic toxins accumulate, subsequently causing renal damage and hypertension, known as the "malignant cycle."[12,40] Accordingly, the reduction of uremic toxins can help protect against renal damage and decrease the progression to ESRD and the need for HD. Renal transporter proteins are potential therapeutic targets for CKD to improve the prognosis of patients with damaged kidneys and some related CVDs.

To understand the mechanism by which SLCO4Cl exerted antihypertensive and anti-inflammation effects, a comprehensive quantitative metabolomic analysis was performed. Blood and urine specimens were measured by CE–MS and high performance liquid chromatography (HPLC). Although the plasma concentration of ADMA, GSA and *trans*-aconitate were significantly increased 3 weeks after the Nx, the increments were significantly decreased in TG(+)Nx rats compared with TG(−)Nx rats (Fig. 3). These data suggest that the excretion of uremic toxins was increased in TG(+) rats.

In CKD patients, the accumulation of uremic toxins causes difficulty in controlling BP, impairs renal function, and worsens the prognosis.[9] Among these toxins, the guanidino compounds GSA and ADMA are increased in CKD patients and correlate with the prognosis.[10–13] It is well known that the accumulation of guanidino compounds (including ADMA and GSA) and several uremic toxins generate oxidative stress causing further renal damage in CKD patients.[65–68]

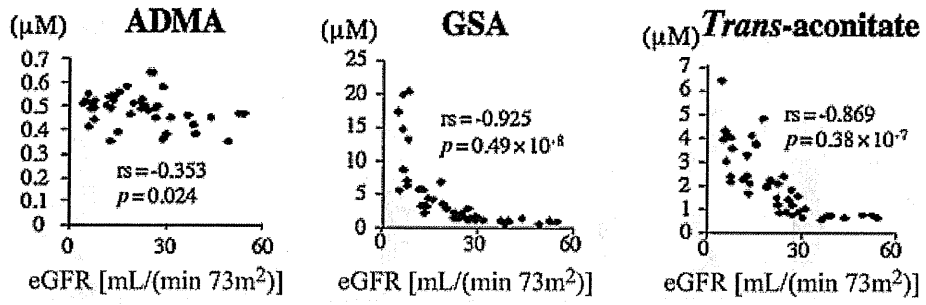

Figure 4. Metabolomic analysis of uremic toxins in patients with CKD. Relation between uremic toxins and eGFR as well as plasma creatinine in 41 CKD patients. Correlation between eGFR and the plasma ADMA, GSA, and trans-aconitate in CKD patients.

In particular, ADMA, an inhibitor of nitric oxide synthase, is implicated in hypertension, renal damage, cardiac hypertrophy, and cardiovascular events.[14,15]

Trans-aconitate is a competitive inhibitor of aconitase.[69] Aconitase is a key enzyme that catalyzes citrate to isocitrate via *cis*-aconitate in the TCA cycle and the accumulation of *trans*-aconitate inhibits the TCA cycle and respiration in tissues.[69] However, the existence of *trans*-aconitate in mammals, its biological effects, and precise role in renal failure have not been clarified. When *trans*-aconitate was administered to rats intraperitoneally, the BP of the injected rats was immediately elevated compared with control.[7] In addition, *trans*-aconitate significantly induced super oxide production in human kidney proximal tubule cells.[7]

Metabolomic Analysis of CKD Patients

To further confirm that not only ADMA and GSA, but also *trans*-aconitate, exist in humans and that their concentrations are increased in accordance with the CKD progression, CE–MS analysis of 41 CKD patients at various stages was performed. The plasma level of *trans*-aconitate was significantly correlated with the increase of plasma creatinine and inversely correlated with the eGFR similar to ADMA and GSA (Fig. 4).[7,8] Because the plasma level of *trans*-aconitate in non-CKD patients is quite low, these data suggest that *trans*-aconitate could serve as a biomarker for predicting the onset of renal damage, and that theelimination of *trans*-aconitate could have a beneficial effect in CKD.

Functional Analysis of SLCO4C1 Promoter and Exploration of Compounds that Enhance SLCO4C1 Expression

Thus, drugs that upregulate SLCO4C1 in the kidney may facilitate the excretion of uremic toxins and reduce renal inflammation decelerating the progression of renal damage and entry of HD. To address this issue, we isolated the promoter region of human SLCO4C1. We identified xenobiotic responsive element (XRE) motifs containing the core sequence 5′-CACGC-3′ at position 126. That sequence is generally recognized by Aryl hydrocarbon receptor (AhR) and AhR nuclear translocator heterodimer,[70] although the flanking sequences are not typical compared with the cyp1a1 XRE motif.[71,72] AhR binds "classical" ligands of such environmental pollutants as halogenated aromatic hydrocarbons [e.g., dioxin, benzopyrene, 3-methylcholanthrene (3-MC)] [73] (Fig. 5a).

Human SLCO4C1 promoter activity was increased by 3-MC. As AhR can also bind to a structurally divergent range of chemicals,[73] we next screened various compounds. Interestingly, the HMG-CoA reductase inhibitors (statin), fluvastatin (2.3-fold at 10 μM), and pravastatin (1.3-fold at 30 μM) upregulated the SLCO4C1 promoter activity (Fig. 5b). Deletion experiments showed that all constructs exerted potent promoter activation but removal of the XRE core segment or mutation in the XRE core motifs abolished the response to fluvastatin.[7] Various clinically available statins, simvastatin, lovastatin, cerivastatin, itavastatin, mevastatin, atorvastatin, rosuvastatin, and pitavastatin upregulate SLCO4C1 transcription.[7] The binding was further characterized by chromatin immunoprecipitation (ChIP) assay. Application of the antibody against AhR resulted in a positive band for both 3-MC and fluvastatin.[7] These data suggested that statins regulate SLCO4C1 transcription through the AhR–XRE system. In human kidney proximal cells, the application of fluvastatin and pravastatin significantly enhanced SLCO4C1 mRNA expression.[7] The uptake of thyroid hormone, T3, a representative substrate of SLCO4C1, was also significantly facilitated by fluvastatin and pravastatin, suggesting potentiation of the SLCO4C1 function in the proximal tubules.[7]

We next examined the effects of pravastatin *in vivo*. Pravastatin was administered to 5/6-nephrectomized (Nx) Wistar rats and the renal tubular function was examined. After the administration of pravastatin, BP was not changed but the mRNA level of

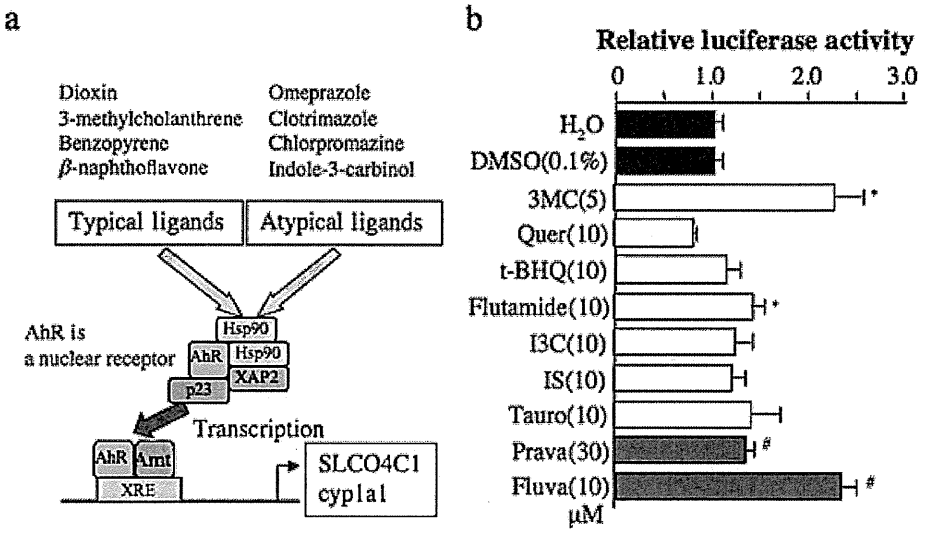

Figure 5. Transcriptional analysis of SLCO4C1 promoter and ligand screening. (a) Typical and atypical ligands of aryl hydrocarbon receptor (AhR) and schematic illustration of AhR–XRE axis of transcriptional regulation. (b) Enhancement of promoter activity of human SLCO4C1 with various compounds (concentration as indicated, μM). Quer, quercetin; t-BHQ, *tert*-butylhydroquinone; I3C, indole-3-carbinole; IS, indoxyl sulfate; Tauro, taurocholic acid; Prava, pravastatin; Fluva, fluvastatin. $^{*}p < 0.05$ compared with dimethyl sulfoxide (DMSO), $^{**}p < 0.05$ compared with H_2O.

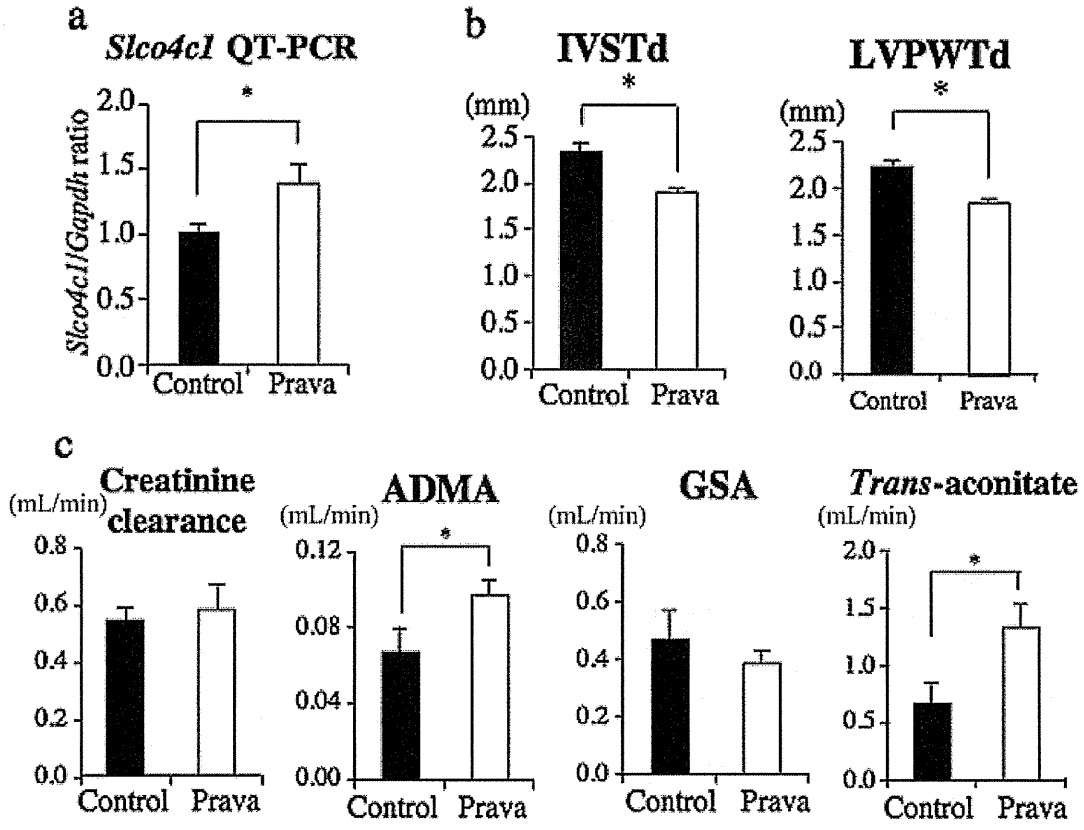

Figure 6. Effects of statins on SLCO4C1 expression and function *in vitro* and *in vivo*. (a) The mRNA expression of rat slco4c1 in the kidney after pravastatin administration. (b) IVSTd and LVPWTd before and after 5/6 nephrectomy. $^{*}P<0.05$. (c) Renal clearance of creatinine, ADMA, *trans*-aconitate, and GSA 3 weeks after 5/6 nephrectomy.

 DOI 10.1002/jps

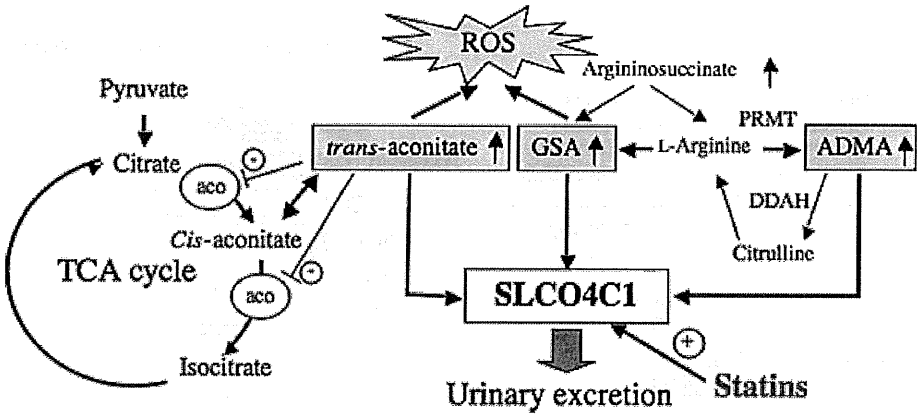

Figure 7. Uremic toxins and SLCO4C1 transporter in renal failure. ADMA is formed by protein ariginine *N*-methyltransferase (PRMT) from arginine and degrades to citrulline by dimethylarginine dimethylaminohydrolase (DDAH). Note that SLCO4C1 facilitates the excretion of GSA, ADMA, and *trans*-aconitate and that statins increase the expression and the function of SLCO4C1 resulting in reductions of the uremic toxins and BP. *Trans*-aconitase inhibits aconitase activity and induces reactive oxygen species (ROS). Aco, aconitase.

rat slco4c1 was significantly increased in the kidney (Fig. 6a) Under this condition, the ADMA and *trans*-aconitate clearance was significantly increased in the pravastatin-treated Nx rats without changing Ccr, although the change in GSA clearance was not statistically significant (Fig. 6c). In addition, cardiac hypertrophy was also decreased in the pravastatin-treated group (Fig. 6b). It is suggested that statins function as a nuclear receptor ligand that recruits the AhR–XRE system and upregulates SLCO4C1 transcription to facilitate the excretion of uremic toxins like a transgene phenotype. Because significantly increased levels of GSA and ADMA were reported in patients with autosomal dominant polycystic kidney disease (ADPKD),[13] our data also support this clinical study and will be a new clue for increasing the protection against renal damage in ADPKD patients.

CONCLUSIONS

Organic anion transporters have been vigorously investigated as key molecules in the regulation of the renal excretion of intrinsic compounds and the pharmacokinetics. Recently, a new finding that OATs and OATPs also carry uremic toxins and regulate renal excretion was reported.[2–7] OATs and OATPs might be involved in the emergence of uremic toxicity and the progression of renal damage. The OAT/SLC22 family mediates the uptake of uremic toxins into various organs and might cause "uremia" aggravating end-organ damage. SLCO4C1 is the only OATP/SLC21/SLCO expressed in human kidney, and it plays a critical role in the renal elimination of urinary-excreted drugs and uremic toxins. An enhancement of the urinary excretion of uremic toxins and the amelioration of end-organ damage were also observed in proximal tubular cell-specific human SLCO4C1-overexpressing TG rat as well as statin-induced SLCO4C1 upregulation rat renal failure models. Further examination in clinical trials is needed to verify the effects of increasing uremic toxin transporter in patients with CKD. Metabolomic analysis enables the comprehensive assessment of known and newly identified uremic toxins in CKD patients, and this method is promising for the exploration of surrogate biomarkers of early renal damage and CVDs. A new therapeutic strategy to regulate the expression and function of renal uremic toxin transporters for the elimination of toxins and use the reduction of candidate uremic toxins as surrogate biomarkers in renal therapy is needed (Fig. 7).

REFERENCES

1. Pritchard JB, Miller DS. 1993. Mechanisms mediating renal secretion of organic anions and cations. Physiol Rev 73:765–796.
2. Mikkaichi T, Suzuki T, Onogawa T, Tanemto M, Mizutamari H, Okada M, Chaki T, Masuda T, Toki T, Eto N, Abe M, Satoh F, Unno M, Hishinuma T, Inui K, Ito S, Goto J, Abe T. 2004. Isolation and characterization of a digoxin transporter and its rat homologue expressed in the kidney. Proc Natl Acad Sci USA 101:3569–3574.
3. Enomoto A, Takeda M, Tojo A, Sekine T, Cha SH, Khamdang S, Takayama F, Aoyama I, Nakamura S, Enou H, Niwa T. 2002. Roles of organic anion transporters in the tubular transport of indoxyl sulfate and the induction of its nephrotoxicity. J Am Soc Nephrol 13:1711–1720.

4. Enomoto A, Takeda M, Taki K, Takayama F, Noshiro R, Niwa T, Endou H. 2003. Interactions of human organic anion as well as cation transporters with indoxyl sulfate. Eur J Phramacol. 466:3–20.
5. Deguch T, Ohtsuki S, Otagiri M, Takanaga H, Asaba H, Mori S, Terasaki T. 2002. Major role of organic anion transporter 3 in the transport of indoxyl sulfate in the kidney. Kidney Int 61:1760–1768.
6. Deguchi T, Kusuhara H, Takadate A, Endou H, Otagiri M, Sugiyama Y. 2004. Characterization of uremic toxin transport by organic anion transporters in the kidney. Kidney Int 65:162–174.
7. Toyohara T, Suzuki T, Morimoto R, Akiyama Y, Souma T, Shiwaku HO, Takeuchi Y, Mishima E, Abe M, Tanemoto M, Masuda S, Kawano H, Hamemura K, Nakayama M, Sato H, Mikkaichi T, Yamaguchi H, Fukui S, Fukumoto Y, Shimokawa H, Inui K, Terasaki T, Goto J, Ito S, Hishinuma T, Rubera I, Tauc M, Fujii-Kuriyama Y, Yabuuchi H, Moriyama Y, Soga T, Abe T. 2009. SLCO4C1 transporter eliminates uremic toxins and attenuates hypertension and renal inflammation. J Am Soc Nephrol 20:2546–2555.
8. Toyohara T, Akiyama Y, Suzuki T, Takeuchi Y, Mishima E, Tanemoto M, Momose A, Toki N, Sato H, Nakayama M, Hozawa A, Ito S, Soga T, Abe T. 2010. Metabolomic profiling of uremic solutes in CKD patients. Hypertens Res 33:944–952.
9. Go AS, Chertow GM, Fan D, McCulloch CE, Hsu CY. 2004. Chronic kidney disease and the risks of death, cardiovascular events, and hospitalization. N Engl J Med 351:1296–1305.
10. Zoccali C. 2008. Asymmetric dimethylarginine: A novel marker of risk and a potential target for therapy in chronic kidney disease. Curr Opin Nephrol Hypertens 17:609–615.
11. Marescau B, Nagels G, Possemiers I, De Broe ME, Becaus I, Billiouw JM, Lornoy W, De Deyn PP. 1997. Guanidino compounds in serum and urine of nondialyzed patients with chronic renal insufficiency. Metabolism 46:1024–1031.
12. Vanholder R, Van Laecke S, Glorieux G. 2008. What is new in uremic toxicity? Periatr Nephrol 23:1211–1221.
13. Torremans A, Marescau B, Kranzlin B, Gretz N, Billiouw JM, Vanholder R, De Smet R, Bouwman K, Brouns R, De Deyn PP. 2006. Biochemical validation of a rat model for polycystic kidney disease: Comparison of guanidino compound profile with the human condition. Kidney Int 69:2003–2012.
14. Zoccali C, Mallamaci F, Maas R, Benedetto FA, Tripepi G, Malatino LS, Catallotti A, Bellanuova I, Böger R; CREED Investigators. 2002. Left ventricular hypertrophy, cardiac remodeling and asymmetric dimethylarginine (ADMA) in hemodialysis patients. Kidney Int 62:339–345.
15. Fliser D, Kronenberg F, Kielstein JT, Morath C, Bode-Böger SM, Haller H, Ritz E. 2005. Asymmetric dimethylarginine and progression of chronic kidney disease: The mild to moderate kidney disease study. J Am Soc Nephrol 16:2456–2461.
16. Parfrey PS, Foley RN. 1999. The clinical epidemiology of cardiac disease in chronic renal failure. J Am Soc Nephrol 10:1606–1615.
17. London GM, Pannier B, Guerin AP, Blacher J, Marchais SJ, Darne B, Metivier F, Adda H, Safar ME. 2001. Alterations of left ventricular hypertrophy in and survival of patients receiving hemodialysis- follow-up of an interventional study. J Am Soc Nephrol 12:2759–2767.
18. Mikkaichi T, Suzuki T, Tanemoto M, Ito S, Abe T. 2004. The organic anion transporter (OATP) family. Drug Metab Pharmacokinet 19:171–179.
19. Hagenbuch B, Meier PJ. 2004. Organic anion transporting polypeptides of the OATP-SLC21 family-phylogenetic classification as OATP-SLCO superfamily, new nomenclature and molecular functional properties. Pflugers Arch 447:653–665.
20. Koepsell H, Endou H. 2004. The SLC22 drug transporter family. Pflugers Arch 447:666–676.
21. Rizwan AN, Burckhardt G. 2007. Organic anion transporters of the SLC22 family—Biopharmaceutical, physiological, and pathological roles. Pharm Res 24:450–470.
22. Inui K, Masuda S, Saito H. 2000. Cellular and molecular aspects of drug transport in the kidney. Kidney Int 58:944–958.
23. Sekine T, Miyazaki H, Endou H. 2006. Molecular physiology of renal organic anion transporters. Am J Physiol Renal Physiol 290:F251–F261.
24. Laouari D, Yang R, Veau C, Blanke I, Friedlander G. 2001. Two apical multidrug transporters, P-gp and MRP2, are differently altered in chronic renal failure. Am J Physiol Renal Pysiol 280:F636–F645.
25. Smeets PH, van Aubel RA, Wouterse AC, Van Den Heuvel JJ, Russel FG. 2004. Contribution of multidrug resistance protein 2 (MRP2/ABCC2) to the renal excretion of *p*-aminohippurate (PAH) and identification of MRP4 (ABCC4) as a novel PAH transporter. J Am Soc Nephrol 15:2828–2835.
26. van Aubel RA, Smeets PH, Peters JG, Bindels RJ, Russel FG. 2002. The MRP4(ABCC4) gene encodes a novel apical organic anion transporter in human kidney proximal tubules—Putative efflux pump for urinary cAMP and cGMP. J Am Soc Nephrol 13:595–603.
27. Sweet DH, Bush KT, Nigam SK. 2001. The organic anion transporter family—From physiology to ontogeny and the clinic. Am J Physiol Renal Physiol 281:F197–F205.
28. Wright SH, Dantzler WH. 2004. Molecular and cellular physiology of renal organic cation and anion transport. Physiol Rev 84:987–1049.
29. van de Water FM, Masereeuw R, Russel FG. 2005. Function and regulation of multidrug resistance proteins (MRPs) in the renal elimination of organic anions. Drug Metab Rev 37:443–471.
30. Anzai N, Kanai Y, Endou H. 2006. Organic anion transporter family—Current knowledge. J Phramcol Sci 100:411–426.
31. Motohashi H, Sakurai Y, Saito H, Masuda S, Urakami Y, Goto M, Fukatsu A, Ogawa O, Inui K. 2002. Gene expression levels and immunolocalization of organic ion transporters in the human kidney. J Am Soc Nephrol 13:866–874.
32. Sekine T, Cha SH, Tsuda M, Apiwattanakul N, Nakajima N, Kanai Y, Endou H. 1998. Identification of multispecific organic anion transporter 2 expressed predominantly in the liver. FEBS Lett 429:179–181.
33. Enomoto A, Takeda M, Shimoda M, Narikawa S, Kobayashi Y, Kobayashi Y, Kobayashi Y, Yamamoto T, Sekine T, Cha SH, Niwa T, Endou H. 2002. Interaction of human organic anion transporters 2 and 4 with organic anion transport inhibitors. J Pharmacol Exp Ther 301:797–802.
34. Kusuhara H, Sekine T, Utsunomiya-Tate N, Tsuda M, Kojima R, Cha SH, Sugiyama Y, Kanai Y, Endou H. 1999. Molecular cloning and characterization of a new multispecific organic anion transporter from rat brain. J Biol Chem 274:13675–13690.
35. Cha SH, Sekine T, Kusuhara H. 2000. Molecular cloning and characterization of multispecific organic anion transporter 4 expressed in the placenta. J Biol Chem 275:4507–4512
36. Enomoto A, Kimura H, Chairoungdua A, Shigeta Y, Jutabha P, Cha SH, Hosoyamada M, Takeda M, Sekine T, Igarashi T, Matsui H, Kikuchi Y, Oda T, Ichiba K, Hosoya T, Shimokata K, Niwa T, Kanai Y, Endou H. 2002. Molecular identification of a renal urate–anion exchanger that regulates blood urate levels. Nature 417:447–452.
37. Ekarantanawong S, Anzai N, Jutbaha P, Miyazaki H, Noshiro R, Takeda M, Kanai Y, Sophasan S, Endou H. 2004. Human organic anion transporter 4 is a renal apical organic anion/decarboylate exchanger in the proximal tubules. J Phramacol Sci 94:297–304.
38. Enomoto A, Endou H. 2005. Roles of organic anion transporters (OATs) and a urate transporter (URAT1) in the pathophysiology of human disease. Clin Exp Nephrol 9:195–205.

39. Anzai N, Kanai Y, Endou H. 2007. New insights into renal transport of urate. Curr Opin Rheumatol 19:151–157.
40. Vanholder R, Smmet RD, Glorieux G, Argilés A, Baurmeister U, Brunet P, Clark W, Gohen G, De Deyn PP, Deppisch R, Descamps-Latscha B, Henle T, Jörres A, Lemke HD, Massy ZA, Passlick-Deetjen J, Rodriguez M, Stegmayr B, Stenvinkel P, Tetta C, Wanner C, Zidek W;European Uremic Toxin Work Group (EUTox). 2003. Review on uremic toxins—Classification, concentration, and interindividual variability. Kidney Int 63:1934–1943.
41. Niwa T. 2001. Indoxyl sulfate . In Textbook of nephrology; Massry SG, Glassock RJ, Eds. 4th ed. Philadelphia: Williams and Willkins, pp 1269–1272.
42. Niwa T. 2010. Indoxyl sulfate is a nephrovascular toxin. J Ren Nutr 20:S2–S6.
43. Niwa T, Ise M. 1994. Indoxyl sulfate, a circulating uremic toxin, stimulates the progression of glomerular sclerosis. J Lab Clin Med 124:96–104.
44. Miyazaki T, Aoyama I, Ise M, Seo H, Niwa T. 2000. An oral sorbent reduces overload of indoxyl sulfate and gene expression of TGF-β1 in ureic rat kidneys. Nephrol Dial Transplant 15:1773–1781.
45. Enomoto A, Niwa T. 2007. Roles of organic anion transporters in the progression of chronic renal failure. Therapeu Apheresis Dial 11:S27–S31.
46. Deguchi T. Takemoto M, Uehara N, Lindup WE, Suenaga A, Otagiri M. 2005. Renal clearance of endogenous hippurate correlates with expression levels of renal organic anion transporters in uremic rats. J Pharamacol Exp Ther 14:932–938.
47. Matsuzaki T, Watanabe H, Yoshitome K, Morisaki T, Hamada A, Nonoguchi H, Konda Y, Tomita K, Inui K, Saito H. 2007. Down regulation of organic anion transporters in rat kidney under ischemia reperfusion -induced acute renal failure. Kidney Int 71:539–547.
48. Schneider R, Sauvant C, Betz B, Otremba M, Fischer D, Holzinger H, Wanner C, Galle J, Gekle M. 2007. Downregulation of organic anion transporters OAT1 and OAT3 correlates with impaired secretion of para-aminohippurate after ischemic acute renal failure in rats. Am J Physiol Renal Physiol 292:F1599–F1605.
49. Morisaki T Matsuzaki T, yokoo K, Kusumoto M, Iwata K, Hamada A, Saito H. 2008. Regulation of renal organic ion transporters in cisplatin-induced acute kidney injury and uremia in rats. Pharm Res 25:2526–2533.
50. Aleksunes LM, Augstine LM, Scheffer GL, Cherrington NJ, Manautou JE. 2008. Renal xenobiotic transporters are differentially expressed in mice following cisplatin treatment. Toxicology 250:82–88.
51. Sun H, Frasseto L, Benet LZ. 2006. Effects of renal failure on drug transport and metabolism. Pharmacol Ther 109:1–11
52. Saito H. 2010. Pathophysiological regulation of renal SLC22A organic ion transporters in acute kidney injury—Pharmacological and toxicological implications. Pharmacol Ther 125:79–91.
53. Sakurai Y, Motohashi H, Ueo H, Masuda S, Saito H, Okuda M, Mori M, Matsuura M, Doi T, Fukatsu A, Ogawa O, Inui K. 2004. Expression levels of renal organic anion transporters (OATs) and their correlation with anionic drug excretion in patients with renal diseases. Pharm Res 21:61–67.
54. Sakurai Y, Motohashi H, Ogasawara K, Terada T, Masuda S, Katsura T, Mori N, Matsuura M, Doi T, Fukatsu A, Inui K. 2005. Pharmacokinetic siginificance of renal OAT3(SLC22A8) for anionic drug elimination in patients with mesangial proliferative glomerulonephritis. Pharm Res 22:2016–2022.
55. Eraly SA, Vallon V, Vaughn DA, Gangoiti JA, Richter K, Nagle M, Monte JC, Rieg T, Truong DM, Long JM, Barshop BA, Kaler G, Nigam SK. 2006. Decreased renal organic anion secretion and plasma accumulation of endogenous organic anions in OAT1 knock-out mice. J Biol Chem 281:5072–5083.
56. Sweet DH, Miller DS, Pritchard JB, Fujiwara Y, Beier DR, Nigam SK. 2002. Impaired organic anion transport in kidney and choroid plexus of organic anion transporter 3 (Oat3 (Slc22a8)) knockout mice. J Biol Chem 277:26934–26943.
57. Vanwert AL, Bailey RM, Sweet DH. 2007. Organic anion transporter 3 (Oat3,Slc22a8) knockout mice exhibit altered clearance and distribution of penicillin G. Am J Physiol Renal Physiol 293:F1332–F1341
58. VanWert AL, Sweet DH. 2008. Impaired clearance of methotrexate in organic anion transporter 3 (Slc22a8) knockout mice—A gender specific impact of reduced folates. Pharm Res 25:453–462
59. Suzuki T, Abe T. 2008. Thyroid hormone transporters in the brain. Cereberum 7:75–83.
60. Abe T, Suzuki T, Unno M, Tokui T, Sadayoshi I. 2002. Thyroid hormone transporters: Recent advances. Trends Endocrinol Metab 13:215–220.
61. Silverstein DM. 2009. Inflammation in chronic kidney disease: Role in the progression of renal and cardiovascular disease. Pediatr Nephrol 24:1445–1452.
62. Sanaka T, Akizawa T, Koide K, Koshikawa S. 2004. Protective effect of an oral adsorbent on renal function in chronic renal failure: Determinants of its efficacy in diabetic nephropathy. Ther Apher Dial 8:232–40.
63. Owada A, Nakao M, Koike J, Ujiie K, Tomita K, Shiigai T. 1997. Effects of oral adsorbent AST-120 on the progression of chronic renal failure: A randomized controlled study. Kidney Int Suppl 63:S188–S190.
64. Soga T, Ohashi Y, Ueno Y, Naraoka H, Tomita M, Nishioka T. 2003. Quantitative metabolome analysis using capillary electrophoresis mass spectrometry. J Proteome Res 2:488–494.
65. Ueda S, Yamagishi S, Matsumoto Y, Fukami K, Okuda S. 2007. Asymmetric dimethylarginine (ADMA) is a novel emerging risk factor for cardiovascular disease and the development of renal injury in chronic kidney disease. Clin Exp Nephrol 11:115–121.
66. Kielstein JT, Zoccali C. 2008. Asymmetric dimethylarginine: A novel marker of risk and a potential target for therapy in chronic kidney disease. Curr Opin Nephrol Hypertens 17:609–615.
67. Taes YE, Marescau B, De Vriese A, De Deyn PP, Schepers E, Vanholder R, Delanghe JR. 2008. Guanidino compounds after creatine supplementation in renal failure patients and their relation to inflammatory status. Nephrol Dial Transplant 23:1330–1335.
68. De Deyn PP, Vanholder R, Eloot S, Glorieux G. 2009. Guanidino compounds as uremic (neuro) toxins. Semin Dial 22:340–345
69. Saffran M, Prado JL. 1949. Inhibition of aconitase by transaconitate. J Biol Chem 180:1301–1309.
70. Fujii-Kuriyama Y, Miura J. 2005. Molecular mechanism of AhR functions in the regulation of cytochrome P450 genes. Biophys Res Commun 228:311–317.
71. Wu L, Whitlock JP Jr. 1993. Mechanism of dioxin action: Receptor–enhancer interactions in intact cells. Nucleic Acids Res 21:119–125.
72. Nioi P, Hayes JD. 2004. Contribution of NAD(P)H: Quinone oxidoreductase 1 to protection against carcinogenesis, and regulation of its gene by the Nrf2 basic-region leucine zipper and the arylhydrocarbon receptor basic helix-loop-helix transcription factors. Mutat Res 555:149–171.
73. Denison MS, Nagy SR. 2003. Activation of the aryl hydrocarbon receptor by structurally diverse exogenous and endogenous chemicals. Annu Rev Pharmacol Toxicol 43:309–334.

Metabolomics
DOI 10.1007/s11306-011-0353-9

ORIGINAL ARTICLE

Non-targeted metabolite profiling in activated macrophage secretion

Masahiro Sugimoto · Hiroshi Sakagami · Yoshiko Yokote · Hiromi Onuma · Miku Kaneko · Masayo Mori · Yasuko Sakaguchi · Tomoyoshi Soga · Masaru Tomita

Received: 29 March 2011 / Accepted: 9 August 2011

Abstract Periodontal diseases are inflammatory infectious diseases that affect the periodontal tissue. Macrophages play a central role in inflammatory conditions, leading to the destruction of tissues. Identifying the signaling molecules secreted by macrophages would be valuable to the study of these diseases. Here, we present non-targeted analysis using capillary electrophoresis time-of-flight mass spectrometry (CE-TOFMS) for the profiling of extracellular metabolites released during macrophage activation. Lipopolysaccharide (LPS)-induced activation of a mouse macrophage-like cell line RAW264.7 was used as a model system. Cells were treated without (control) or with LPS for 22 h and, after washing, were incubated for 1 h in phosphate-buffered saline. The accumulation of metabolites in the culture supernatant was monitored. LPS treatment significantly enhanced the accumulation of prostaglandins, tumor necrosis factor-α, nitric oxide and citrulline in the culture medium. RAW264.7 cells produced 46 metabolites and 66% of these showed significant changes ($P < 0.05$) following cell activation. In particular, the production of leucine, hypoxanthine, choline, putrecine, N_8-acetylspermidine, succinate, itaconate, and 4-methyl-2-oxopentanoate was significantly increased by cell activation ($P < 0.001$). Significantly elevated production of lactate and glycine was also observed. Here, we present the first catalog of the up and down-regulation of the various metabolites secreted by macrophages following inflammatory activation.

Keywords Macrophage activation · Lipopolysaccharide · RAW264.7 cells · Capillary electrophoresis-mass spectrometry

1 Introduction

Periodontal disease and its milder form, gingivitis, affects 50–90% of adults worldwide, depending on the precise definition of the disease (Pihlstrom et al. 2005). The disease results in the destruction of periodontal tissues and the supporting dental structure, and is associated with systemic diseases such as diabetes, cancer, cardiovascular disease, and preterm birth (Meyer et al. 2008). Periodontal diseases are caused by complex interactions between the host tissue and bacteria at the junctional and crevicular epithelia, and is mainly mediated by the host's response to bacteria (Van Dyke and Serhan 2003).

Neutrophils and macrophages play important roles in the innate inflammatory response during the progression of periodontal disease, with sequential events being triggered by lipopolysaccharide (LPS) from gram-negative bacteria at the tooth root surface. Polymorphonuclear leukocytes are

M. Sugimoto and H. Sakagami contributed equally to this work.

M. Sugimoto (✉) · H. Onuma · M. Kaneko · M. Mori · Y. Sakaguchi · T. Soga · M. Tomita
Institute for Advanced Biosciences, Keio University, Tsuruoka, Yamagata 997-0017, Japan
e-mail: msugi@sfc.keio.ac.jp

M. Sugimoto · T. Soga · M. Tomita
Systems Biology Program, Graduate School of Media and Governance, Keio University, Fujisawa, Kanagawa 252-8520, Japan

H. Sakagami
Divisions of Pharmacology, Meikai University School of Dentistry, Sakado, Saitama 350-0283, Japan

Y. Yokote
Faculty of Science, Josai University, Sakado, Saitama 350-0295, Japan

Published online: 24 August 2011

recruited to the site, and monocytes and activated macrophages respond to endotoxin by releasing various cytokines and interleukin-1β, which stimulates further tissue destruction (Giannobile et al. 2009). Therefore, understanding the biochemical cascades induced by macrophages is important for the diagnosis and treatment of periodontal diseases.

Macrophages perform a multitude of functions essential for tissue remodeling and the immune response, and produce a wide array of pro-inflammatory cytokines, growth factors, lysozymes, proteases, complement components, coagulation factors and prostaglandins upon stimulation with LPS or hypoxic stress (Bingle et al. 2002). A mouse macrophage-like cell line (RAW264.7) (Ralph and Nakoinz 1977) has been used by many investigators in experiments designed to elucidate the signal transduction events during macrophage activation. Using this cell line, we have previously profiled amino acid release and found that the extracellular levels of glycine were significantly elevated during LPS-induced activation (Nishiyama et al. 2010). Glycine is the most abundant amino acid found in saliva (Nakamura et al. 2010) and salivary glycine levels are significantly elevated in elderly persons regardless of gender (Tanaka et al. 2010). This suggests that activated macrophages may be involved in age-related changes to salivary composition. Elevated levels of glycine in the saliva of elderly persons may aggravate periodontitis by stimulating the production of prostaglandin E_2 and cyclooxygenase-2 (COX-2) protein by interleukin-1β-stimulated human gingival fibroblast cells (Rausch-Fan et al. 2005). However, the importance of changes in glycine levels relative to other intracellular metabolite changes induced in activated macrophages remains unclear.

Metabolomics, the simultaneous quantification of all intercellular or intracellular metabolites, has become a powerful new tool that can provide insight into cellular functions (Soga et al. 2003). Several metabolites have been identified as endogenous chemical mediators that orchestrate the host's response in periodontal diseases. These metabolites include lipid-derived mediators, key inflammation signaling molecules (Van Dyke and Serhan 2003), and adenosine and inosine (Cronstein et al. 1999a, b), which are upregulated by cells in response to stress. Although the metabolite profiles of individual pathways, including lipid (Van Dyke and Serhan 2003), amino acid (Li et al. 2007) and carbohydrate (Rodriguez-Prados et al. 2010) metabolites, have been revealed, a broad understanding of these metabolomic profiles is necessary to determine the pathogenic mechanisms involved in innate macrophage inflammation in periodontal diseases.

In this study, we present the first comprehensive metabolomic analysis of the culture supernatants of unstimulated and stimulated macrophage cells to identify the metabolites secreted from macrophages at inflammatory sites such as periodontal tissues during periodontal disease. To profile a wide range of metabolites, non-targeted analyses of the extracellular environment of RAW264.7 cells treated without and with LPS were conducted using capillary electrophoresis time-of-flight mass spectrometry (CE-TOFMS) (Soga et al. 2006).

2 Materials and methods

2.1 Materials

Dulbecco's modified Eagle medium (DMEM) was purchased from GIBCO BRL (Grand Island, NY, USA), fetal bovine serum (FBS) was from JRH Biosciences (Lenexa, KS, USA) and LPS from *E. coli*, Serotype 0111:B4 was purchased from Sigma (St. Louis, MO, USA). Ophthalmate was purchased from Bachem AG (Bubendorf, Switzerland). Acetohydroxamate and azetidine-2-carboxylate were purchased from Chem Service (West Chester, PA, USA). Glucose 1-phosphate and 5-aminovalerate were purchased from Fluka (Buchs, Switzerland). Betaine was purchased from Tokyo Chemical Industry (Tokyo, Japan). All other compounds were purchased from Sigma-Aldrich (St. Louis, MO, USA) or Wako (Osaka, Japan).

2.2 Cell culture

Mouse macrophage-like RAW264.7 cells (purchased from Dainippon Sumitomo Pharma, Osaka, Japan) were cultured at 37°C in DMEM supplemented with 10% FBS under a humidified 5% CO_2 atmosphere.

2.3 LPS activation

Cells (8×10^5 cells/ml, 2 ml) were inoculated on a six-well plate (Becton–Dickinson, Labware, NJ, USA) and incubated at 37°C for 4 h for the cells to completely adhere to the plate. The medium was changed with fresh medium and the cells were then incubated for 22 h without (LPS−) or with 100 ng/ml LPS (LPS+). The experiment was carried out in triplicate. The cells were washed twice with phosphate-buffered saline without calcium or magnesium (PBS−), and then incubated in 1 mL of PBS−. An aliquot (0.5 ml) was removed immediately from each well to provide samples to analyze the initial metabolite mixture, and the cells were then incubated for 60 min at 37°C with the remaining 0.5 ml of PBS− in a 5% CO_2 incubator. All samples were centrifuged (10,000×g, 60 min) through a 3-kDa cutoff filter (Pall Corporation, NY, USA) to remove macromolecules, and the filtrates were assayed to detect nitric oxide (NO), tumor necrosis factor-α (TNF-α), amino acids and other cellular metabolites as described below.

A short incubation time (60 min) was used to minimize cell damage during incubation in PBS−. After incubation, the number of viable cells, which were not stained with 0.15% trypan blue in PBS−, was counted using a hemocytometer under a light microscope. The production rate for each compound was determined by subtracting the initial value from the value obtained after 60 min incubation, and expressed as nmol/10^6 cells/h.

2.4 NO assay

Since NO is a highly unstable compound, NO present in the culture medium was detected directly, without centrifugation, using the Griess method (Takahashi et al. 2008).

2.5 TNF-α assays

The culture supernatants were assayed using an ELISA kit (R&D Systems Inc, Minneapolis, MN, USA) to measure the concentration of TNF-α. The assay was performed according to the manufacturer's instructions.

2.6 Sample preparation for CE-TOFMS

To 100 μl of the extracellular-dissolved samples, 400 μl of methanol containing internal standards (50 μmol/l each of methionine sulfone, 2-[*N*-morpholino]-ethanesulfonic acid, and D-camphor-10-sulfonic acid) was added. The homogenate was then mixed with Milli-Q water and chloroform at a volume ratio of 5:2:5, and the mixture was centrifuged at 20,400×*g*, for 15 min at 4°C. The aqueous layer was filtered to remove macromolecules by centrifugation through a 5-kDa cutoff filter (Millipore) at 9,100×*g* for 2.5 h at 4°C. The filtrate (300 μl) was concentrated by centrifugation and dissolved in 50 μl of Milli-Q water containing reference compounds (200 μmol/l each of 3-aminopyrrolidine and trimesate) immediately before CE-TOFMS analysis.

2.7 Instrumental parameters for CE-TOFMS

The instrumentation and measurement conditions used for CE-TOFMS are described elsewhere (Sugimoto et al. 2010a; Soga et al. 2006, 2009). Cation analysis was performed using an Agilent CE capillary electrophoresis system, an Agilent G6220A LC/MSD TOF system, an Agilent 1100 series isocratic HPLC pump, a G1603A Agilent CE-MS adapter kit, and a G1607A Agilent CE-ESI-MS sprayer kit (Agilent Technologies, Waldbronn, Germany). Anion analysis was performed using an Agilent CE capillary electrophoresis system, an Agilent G6210A LC/MSD TOF system, an Agilent 1200 series isocratic HPLC pump, a G1603A Agilent CE-MS adapter kit and a G1607A Agilent CE-electrospray ionization (ESI) source-MS sprayer kit (Agilent Technologies). For both the cation and anion analyses, the CE-MS adapter kit includes a capillary cassette that enables thermostatic control of the capillary. The CE-ESIMS sprayer kit simplifies coupling of the CE system with the MS systems and is equipped with an electrospray source. For system control and data acquisition, we used G2201AA Agilent ChemStation software for CE and Agilent MassHunter software for TOF-MS. For anion analysis, the original Agilent SST316Ti stainless steel ESI needle was replaced with a SST316Ti stainless steel and platinum needle, which was passivated using 1% formic acid and 20% isopropanol aqueous solution at 80°C for 30 min.

For cationic metabolite analysis using CE-TOFMS (Soga et al. 2006), the samples were separated in fused silica capillaries (50 μm i.d. × 100 cm total length) filled with 1 mol/l formic acid as the reference electrolyte. Sample solutions were injected at 50 mbar for 3 s and a voltage of 30 kV was applied. The capillary temperature was maintained at 20°C and the temperature of the sample tray was kept below 5°C. The sheath liquid, composed of methanol/water (50% v/v) and 0.1 μmol/l hexakis (2,2-difluoroethoxy) phosphazene (Hexakis), was delivered at 10 μl/min. ESI-TOF-MS was conducted in the positive ion mode. The capillary voltage was set at 4 kV and the flow rate of nitrogen gas (heater temperature = 300°C) was set at 10 psig. In TOF-MS, the fragmentor, skimmer and OCT RF voltages were set at 75, 50 and 125 V, respectively. Automatic recalibration of each acquired spectrum was performed using reference masses of reference standards {[^{13}C isotopic ion of protonated methanol dimer $(2MeOH + H)]^+$, *m/z* 66.063061) and ([protonated Hexakis $(M + H)]^+$, *m/z* 622.02896}. Mass spectra were acquired at the rate of 1.5 cycles/s over a *m/z* range of 50–1,000.

For anionic metabolite analysis using CE-TOFMS (Soga et al. 2009), a commercially available COSMO(+) capillary (50 μm i.d. × 110 cm, Nacalai Tesque, Kyoto, Japan), chemically coated with a cationic polymer, was used for separation. A 50-mmol/l ammonium acetate solution (pH 8.5) was used as the electrolyte to achieve separation. Before the first use, a new capillary was flushed successively for 10 min each with the running electrolyte (pH 8.5), 50 mmol/l acetic acid (pH 3.4), and then the electrolyte again. Before each injection, the capillary was equilibrated for 2 min by flushing with 50 mM acetic acid (pH 3.4) and then for 5 min by flushing with the running electrolyte. A sample solution (30 nl) was injected at 50 mbar for 30 s, and a voltage of −30 kV was applied. The capillary temperature was maintained at 20°C and the sample tray was cooled below 5°C. An Agilent 1100 series pump equipped with a 1:100 splitter was used to deliver 5 mM ammonium acetate in 50% (v/v) methanol/water, containing 0.1 μM Hexakis to the CE interface at 10 μl/min. Here,

it was used as a sheath liquid around the outside of the CE capillary to provide a stable electrical connection between the tip of the capillary and the grounded electrospray needle. ESI-TOF-MS was conducted in negative ionization mode with the capillary voltage set to 3,500 V. For TOF-MS, the fragmentor, skimmer and Oct RF voltages were set at 100, 50 and 200 V, respectively. The flow rate of the drying nitrogen gas (heater temperature = 300°C) was 10 l/min. Automatic recalibration of each acquired spectrum was performed using reference masses of reference standards {[^{13}C isotopic ion of deprotonated acetic acid dimer (2 $CH_3COOH–H)]^-$, *m/z* 120.038339}, and {[Hexakis-deprotonated acetic acid ($CH_3COOH–H)]^-$, *m/z* 680.03554)}. Exact mass data were acquired at a rate of 1.5 spectra/s over a *m/z* range of 50–1,000.

2.8 Sample preparation for LC-TOFMS

To 30 µl of the extracellular samples, 270 µl of isopropyl alcohol containing an internal standard (2.2 µmol/l of camphor-10-sulfonic acid) was added with shaking. The mixture was centrifuged at 20,400×*g* for 10 min at 4°C, and the supernatant was then transferred to another tube and vacuum dried at 35°C. The samples were mixed with chloroform, methanol, and Milli-Q water in a volume ratio of 2:4:1 containing 20 µmol/l of 3,5-di-*tert*-butyl-4-hydroxyhydrocinnamate, centrifuged at 20,400×*g*, for 5 min at 4°C, and 25 µl of the supernatant was used for LC-TOFMS analysis.

2.9 LC-TOFMS parameters

The LC system was an Agilent 1290 infinity HPLC (Agilent Technologies). The Acquity UPLC® BEH C18 (1.7 µm), φ 2.1 × 50 mm column was purchased from Waters (Tokyo, Japan), and was maintained at 50°C. The mobile phase consisted of 0.5% acetic acid/water as eluent A and isopropanol as eluent B. A gradient of 1–99% B over 12 min was used, followed by isocratic elution at 99% for a further 17 min. The flow rate was 0.3 ml/min and the injection volume was 1 µl.

MS data were acquired on a 6530 Accurate-Mass Q-TOF LC/MS using the dual spray ESI of G-3251A (Agilent). Samples were analyzed by both positive and negative ion electrospray mass spectrometry. The MS conditions used were as follows: gas temperature 350°C, drying gas 10 l/min, nebulizer 30 psig, fragmentor 200 V, skimmer 90 V, OCT1 RF Vpp 250 V, scan range *m/z* 100–1,600 and nozzle voltage 1,000 V. The capillary voltages were 3.5 and 4.0 kV for negative and positive mode, respectively.

2.10 Determination of free amino acids

The culture medium (0.1 ml) was mixed with 0.1 ml of 10% trichloroacetic acid (Wako). After centrifugation for 5 min at 21,000×*g* at 4°C, the deproteinized supernatant was collected and stored at −30°C. The supernatants (20 µl) were analyzed using a JLC-500/V amino acid analyzer (JEOL, Tokyo, Japan) and amino acids were detected by the ninhydrin reaction (Yamazaki et al. 2007).

2.11 Data and statistical analysis

Raw data were analyzed using our proprietary software called MasterHands, which detected all possible peaks, eliminated noise and redundant features, and generated the aligned data matrix, including annotated metabolite identities and relative areas (peak areas normalized via comparison with internal standards) (Sugimoto et al. 2010b). Concentrations were calculated using external standards based on relative areas. Student's *t* test (two-tailed) was used for statistical comparisons.

3 Results and discussion

3.1 Overview of the metabolomic profiles

In total, CE-TOFMS identified 44 charged metabolites secreted by macrophages (Fig. 1; Table 1). Prostaglandin E_2 and $F_2\alpha$ were observed by LC-TOFMS as they were not charged and therefore not detected by CE-TOFMS. However, because of their similar molecular structures, these two metabolites could not be adequately resolved by LC-TOFMS, so only their combined production could be calculated and used in subsequent analyses.

3.2 Validation of the amino acid profiles determined by CE-TOFMS and the amino acid analyzer

The quantified amino acids were validated by comparing the amino acids profiles consistently obtained by CE-TOFMS with those obtained using an amino acid analyzer (Fig. 2). The metabolites present at high concentrations, such as glycine, alanine and threonine, showed slightly greater discrepancy between the profiles determined by the two methods than metabolites present at low concentrations. Nevertheless, reasonably high overall correlation coefficients were obtained for the unstimulated and LPS-stimulated macrophages, which were $R = 0.855$ ($P < 0.0001$, Pearson correlation) and $R = 0.928$ ($P < 0.0001$, Pearson correlation), respectively.

3.3 Stimulatory effect of LPS on macrophages

NO production by stimulated RAW264.7 cells was significantly increased from 0.20 to 0.66 nmol/10^6 cells/h (3.3-fold increase, $P = 0.0002$) (Fig. 3a), and TNF-α production was also significantly increased from 21.7 to 682.5 pg/10^6 cells/h

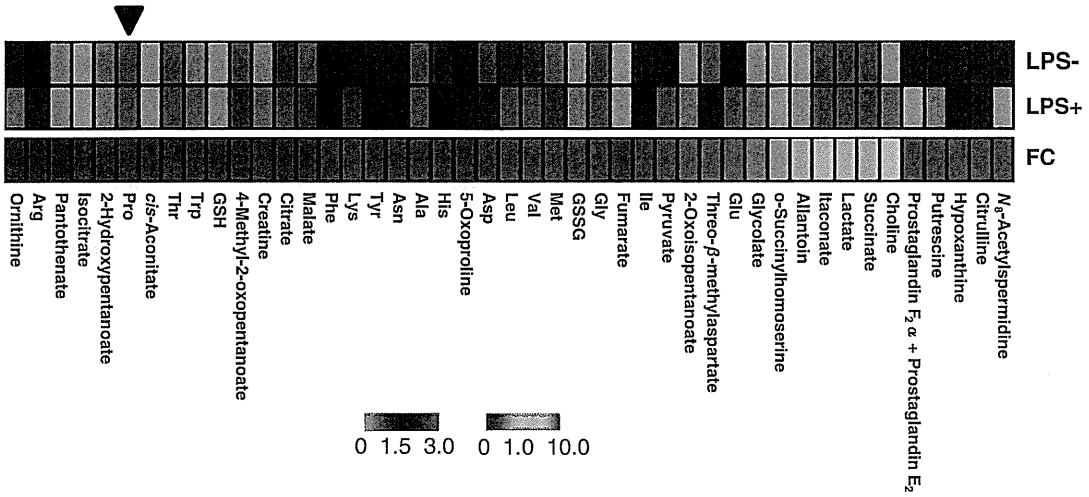

Fig. 1 *Heatmap* and *bar graph* visualization of the quantified metabolites. *Heatmap* showing the quantified metabolites using a *green–black–red scheme*, and the fold-change of metabolites in LPS+ versus LPS− cells. Where metabolites were not detected in LPS− cells, a 10-fold change was allocated. Proline, marked with *triangle*, showed no change. *FC* fold change

(31.5-fold increase, $P = 0.0151$) (Fig. 3b). Citrulline production, which accompanies NO production at a molar ratio of 1:1, is generated from arginine by inducible NO synthase (Paradise et al. 2010). It was only observed for stimulated RAW264.7 cells (2.19 nmol/10^6 cells/h, $P = 3.0 \times 10^{-5}$) (Table 1). Since NO is labile, citrulline levels are a more reliable guide to the levels of NO synthase activity. These data confirmed that LPS activated the RAW264.7 cells.

Prostaglandin E_2 and $F_2\alpha$, detected by LC-TOFMS, are central molecules in inflammatory processes. The inflammatory response of macrophages induces prostanoid synthesis by (1) inducing mobilization of the fatty acid substrate arachidonate from membrane phospholipids, (2) promoting prostaglandin H_2 production from arachidonate by upregulating cyclooxygenases 1 and 2 (COX-1/2), and (3) converting prostaglandin H_2 to specific prostanoids, such as prostaglandin E_2 and $F_2\alpha$ (Noguchi and Ishikawa 2007). The production of prostaglandin E_2 and $F_2\alpha$ (4.6×10^{-3} nmol/10^6 cells/h, $P = 1.2 \times 10^{-6}$) was only observed in stimulated RAW264.7 cells, again confirming the activation of these macrophages.

3.4 Amino acid profiles of stimulated macrophages

3.4.1 Glycine, serine and cysteine production

In amino acid profiles, glycine production was the highest of all amino acids detected (LPS− vs. LPS+: 17.1 vs. 29.5 nmol/10^6 cells/h, $P = 0.073$) (Table 1), which is consistent with previous studies using LPS-stimulated mouse macrophages and regular culture medium (DMEM + 10% FBS) (Nishiyama et al. 2010). Glycine has been reported to stimulate the production of prostaglandin E_2 and COX-2 protein in interleukin-1β-stimulated human gingival fibroblast cells, suggesting its involvement in the pathogenesis of periodontitis (Rausch-Fan et al. 2005). On the other hand, glycine has been reported to inhibit the production of inflammatory cytokines by macrophages by blocking calcium channels (Rose et al. 1999), inhibiting TNF-α secretion and increasing IL-10 production (Xu et al. 2008), or via neutral amino acid transporters (Carmans et al. 2010). Glycine inhibited the growth of an endothelial cell line (Yamashina et al. 2007) and salivary gland-derived progenitor cells (Nakamura et al. 2009). Although these data are contradictory, they mostly suggest that glycine negatively regulates the growth and activation of various cultured cells. This metabolite is also the most abundant amino acid in the saliva (Takeda et al. 2009; Tanaka et al. 2010); however, the cells in the oral cavity that secrete glycine have not been identified. In association with glycine pathway, serine, a major source of glycine, was only detected by the amino acid analyzer, but was present at relatively low concentrations (Table 1; LPS− vs. LPS+: 1.0 ± 0.074 vs. 1.1 ± 0.12 nmol/10^6 cells/h, 1.1 fold). Cysteine, which is synthesized from serine, was not observed, possibly due to the limited supply of serine.

3.4.2 Glutamate, glutamine, proline and arginine production

Glutamate, a key intermediate in amino acid metabolism, including biosynthetic and degradative pathways, is formed from α-ketoglutarate in the tricarboxylic acid (TCA) cycle. We found that glutamate production was increased by 2.2-fold ($P = 0.0043$) in activated macrophages, and its

Table 1 Profiled metabolites of RAW264.7 cells

Mode	Metabolite	LPS−		LPS+		*P* value	FC
		Mean	SD	Mean	SD		
C	Gly	17.1	7.79	29.4	4.21	0.0735	1.7
C	Ala	8.61	1.65	13.1	3.19	0.0988	1.5
C	Thr	7.50	0.594	9.13	0.501	0.0219	1.2
C	Pro	4.17	0.385	4.22	0.323	0.891	1.0
C	Val	2.50	0.424	4.18	0.361	6.41×10^{-3}	1.7
C	Leu	2.25	0.227	3.75	0.153	6.80×10^{-4}	1.7
C	Glu	1.48	0.0657	3.28	0.530	4.31×10^{-3}	2.2
C	Lys	1.72	0.231	2.54	0.337	0.0251	1.5
C	Cit	0.00	0.00	2.19	0.180	3.01×10^{-5}	N.A
C	Ile	1.04	0.232	1.86	0.0675	4.19×10^{-3}	1.8
C	Phe	1.27	0.180	1.86	0.182	0.0162	1.5
C	Asn	1.14	0.194	1.72	0.222	0.0275	1.5
C	Tyr	1.07	0.182	1.61	0.101	0.0111	1.5
C	His	0.970	0.0954	1.48	0.186	0.0134	1.5
C	Asp	0.630	0.119	1.03	0.477	0.235	1.6
C	Arg	1.62	0.196	0.958	0.0862	6.01×10^{-3}	0.59
C	Met	0.482	0.160	0.822	0.0944	0.0340	1.7
C	Trp	0.334	0.0286	0.446	0.0218	5.81×10^{-3}	1.3
C	Hypoxanthine	0.00	0.00	1.22	0.0797	1.21×10^{-5}	N.A.
C	5-Oxoproline	1.34	0.213	2.05	0.310	0.0311	1.5
C	Choline	0.0554	2.52×10^{-3}	0.408	0.0101	5.13×10^{-7}	7.4
C	Creatine	0.287	0.0418	0.401	0.0696	0.0715	1.4
C	Ornithine	1.04	0.239	0.383	0.109	0.0123	0.37
C	Putrescine	0.00	0.00	0.315	0.0605	8.36×10^{-4}	N.A.
C	Allantoin	0.0342	0.415	0.129	2.41	0.950	3.8
C	*o*-Succinylhomoserine	0.0142	0.0480	0.0475	0.0318	0.373	3.3
C	N_8-Acetylspermidine	0.00	0.00	0.0277	2.52×10^{-3}	4.55×10^{-5}	N.A.
C	GSSG	0.217	0.0323	0.371	0.0667	0.0225	1.7
C	GSH	0.118	0.0233	0.164	0.0883	0.428	1.4
A	Glycolate	0.142	0.935	0.367	0.240	0.359	2.6
A	Pyruvate	1.91	0.958	3.66	0.632	9.38×10^{-3}	1.9
A	Lactate	6.65	3.36	37.0	7.58	2.33×10^{-3}	5.6
A	Fumarate	0.0676	0.110	0.117	0.0289	0.291	1.7
A	2-Oxoisopentanoate	0.171	0.238	0.370	0.0370	0.0875	2.2
A	Succinate	0.513	0.237	3.16	0.400	3.30×10^{-4}	6.2
A	2-Hydroxypentanoate	0.379	0.198	0.328	0.0575	0.525	0.86
A	Itaconate	0.549	0.269	2.86	0.254	1.18×10^{-4}	5.2
A	4-Methyl-2-oxopentanoate	0.509	0.256	0.711	0.0391	4.20×10^{-3}	1.4
A	Malate	0.479	0.243	0.680	0.0800	0.0363	1.4
A	Threo-β-methylaspartate	0.511	0.286	1.13	0.0967	1.33×10^{-3}	2.2
A	*cis*-Aconitate	0.114	0.0579	0.123	0.0154	0.562	1.1
A	Isocitrate	0.0520	1.31	0.0444	0.0386	0.761	0.85
A	Citrate	2.62	1.32	3.69	0.485	0.0357	1.4
A	Pantothenate	0.240	0.121	0.184	0.0315	0.0818	0.77

Table 1 continued

Mode	Metabolite	LPS−		LPS+		*P* value	FC
		Mean	SD	Mean	SD		
N	Prostaglandin $F_2\alpha$+ Prostaglandin E_2	0.00	0.00	4.62×10^{-3}	1.68×10^{-4}	1.16×10^{-6}	N.A.

Units are nmol/10^6 cells/h. The metabolite concentraton in LPS− cells was 0 nmol/10^6 cells/h

SD standard deviation; *FC* fold-change; *C* cationic; *A* anionic; *N* neutral; *NA* not applicable

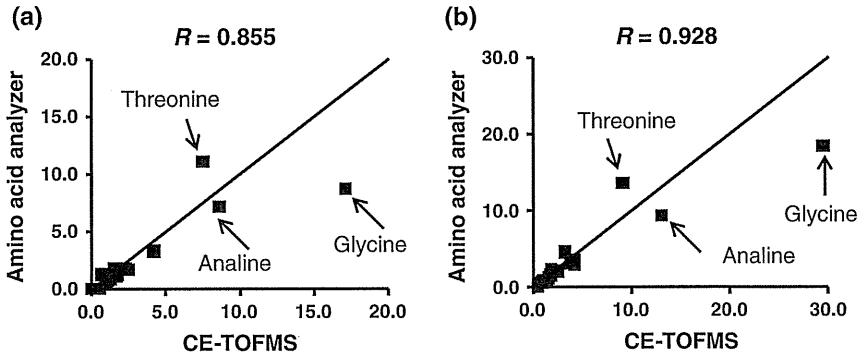

Fig. 2 Comparison of amino acid productions determined by CE-TOFMS and the amino acid analyzer for LPS− (**a**) and LPS+ macrophages (**b**). Units for both *X*- and *Y*-axis are nmol/10^6 cells/h

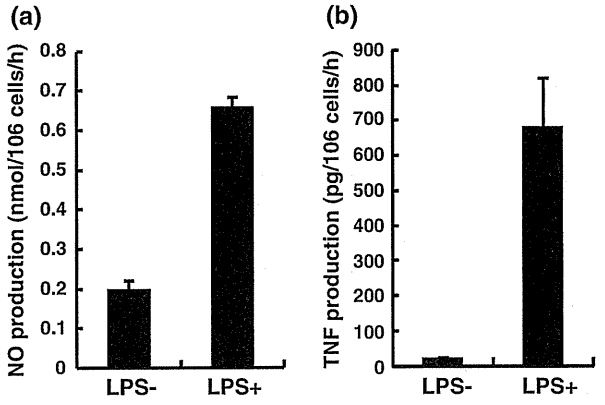

Fig. 3 Stimulation of NO (**a**) and TNF-α (**b**) production in LPS-activated RAW264.7 cells. Values are means ± standard deviation of triplicate determinations

fold-change in production was the highest observed for any amino acid. Glutamate is an excitatory neurotransmitter and the glutamate receptor protein is present on the macrophage cell surface (Noda et al. 2000). Glutamate plays a number of roles in the immune system including removal of oxidants and regulation of immune response (Li et al. 2007). Increased glutamate production in LPS-activated macrophages has already been reported (Stuckey et al. 2005). Glutamate is also a substrate in the synthesis of γ-aminobutyrate (GABA), present in macrophages (Stuckey et al. 2005). However, in this study, GABA was not detected in the culture supernatant of the activated macrophages.

Proline is synthesized from glutamate, but its concentration did not change, despite LPS stimulation (1.0-fold, $P = 0.891$). In contrast, significant decreases in arginine (0.59-fold, $P = 6.01 \times 10^{-3}$) and ornithine (0.37-fold, $P = 0.109$) were observed; ornithine is synthesized from arginine by arginase. Considering the excessive increase of citrulline upon macrophage activation, the arginine pathway seems to be highly activated and mainly used for citrulline synthesis,

3.4.3 Production of other amino acids

The production of alanine (1.5-fold, $P = 0.0988$), valine (1.7-fold, $P = 6.41 \times 10^{-3}$), and leucine (1.7-fold, $P = 6.80 \times 10^{-4}$) was increased to a similar extent by macrophage activation. The production of pyruvate, their precursor metabolite, was also elevated (1.9-fold, $P = 9.38 \times 10^{-3}$). Thus, the change of these metabolites might be due to pyruvate elevation. Aspartate (1.6-fold), which is formed from the TCA component oxaloacetate by the action of transaminase, and its downstream metabolites such as asparagine, lysine, methionine, threonine, isoleucine (from 1.2 to 1.8-fold), showed similar upregulation (Fig. 4; Table 1). On the other hand, cysteine was undetected, probably because of its degradation during sample preparation before CE-TOFMS.

3.5 Metabolomic profile of carbohydrate metabolism

3.5.1 Lactate production

Lactate production in activated macrophages was significantly elevated, and this elevation was the largest observed of all metabolites (37.0 nmol/10^6 cells/h, 5.57-fold increase, $P = 0.0023$). This finding is consistent with previous reports showing that glycolysis and lactate production were increased during osteoclast differentiation induced by receptor activator of nuclear factor [NB]-κB ligand (RANKL) in RAW264.7 cells (Kim et al. 2007). The increase in lactate production, the end product of monooxidative glycolysis, indicates that the glycolysis pathway is activated. Enhanced glycolysis in macrophages is likely to be a survival strategy to cope with the low oxygen conditions commonly observed at inflammatory lesions (Roiniotis et al. 2009). Lactate is a signaling molecule that can activate macrophages by stimulating inflammatory pathways, such as the TLR4 and NF-κB pathways (Samuvel et al. 2009; Nareika et al. 2005). Combined stimulation with LPS and lactate was shown to enhance macrophage activation more than LPS alone (Samuvel et al. 2009). The positive correlation between lactate production and macrophage activation observed here suggests an interaction between extracellular lactate and macrophages, possibly by a feed-forward loop, although further studies are necessary to confirm this postulation.

3.5.2 The balance between glycolysis and TCA cycle activation

Although less substantial than the change in lactate production, a significant increase in TCA cycle metabolite production was observed following macrophage activation. The levels of citrate, succinate, itaconate, malate and fumarate all increased following activation (Table 1). Rodriguez-Prados et al. (2010) observed upregulation of genes involved in glycolysis and downregulation of genes involved in the TCA cycle of LPS-activated macrophages. Indeed, the production of pyruvate in our study was significantly increased (1.9-fold, $P = 0.0094$). It is plausible that glycolysis was activated in activated macrophages under conditions where overall energy metabolism was enhanced. This implies that, even though genes in the TCA cycle were downregulated, the excessive activation of glycolysis caused a slight increase in several metabolites of the TCA cycle.

3.6 Oxidative stress

Barnes et al. (2009) found that the levels of hypoxanthine, inosine, xanthine, guanosine and guanine in gingival crevicular fluid (GCF) were elevated in inflammation sites compared with healthy sites in a human oral cavity. Their findings suggest accelerated activity of the purine degradation pathway and the production of reactive oxygen species causing marked cellular oxidative stress. In this study, we only detected hypoxanthine in activated macrophages (1.22 nmol/10^6 cells/h, $P = 1.2 \times 10^{-5}$).

GSH plays an anti-inflammatory role via its role as an antioxidant (Ghezzi 2011). The production of GSH was increased slightly (1.4-fold, $P = 0.43$), while the production of GSSG was significantly increased after activation in this study (1.7-fold, $P = 0.022$). The ratio of GSH and GSSG decreased slightly from 0.54 to 0.44 ($P = 0.64$) but this decrease was at levels below those considered significant, indicating no dramatic change in oxidative stress after treating macrophages with LPS. Allantoin, which is a uric acid oxidation product, and is therefore a marker for oxidative stress (Kand'ar et al. 2006), also showed no significant changes following exposure to LPS (3.8-fold, $P = 0.95$). These findings conflict with the elevated production of hypoxanthine, a marker for oxidative stress. Therefore, the profiling of cellular metabolites and integration of those data with the extracellular profiles determined in this study would be valuable.

3.7 Other metabolites secreted by macrophages

In addition to amino acids and metabolites related to energy metabolism, several other metabolites were also identified. The production of threo-β-methylaspartate, which is generated from oxaloacetate and NH_3 via threo-3-hydroxy-L-aspartate ammonia-lyase, was significantly increased following activation (2.2-fold, $P = 0.0013$). N_8-Acetylspermidine ($P = 4.5 \times 10^{-5}$, not detected in LPS− cells), a polyamine that generally indicates active cell growth, was only detected in activated macrophages. While the increases following activation were statistically significant ($P > 0.05$) for the following metabolites, there

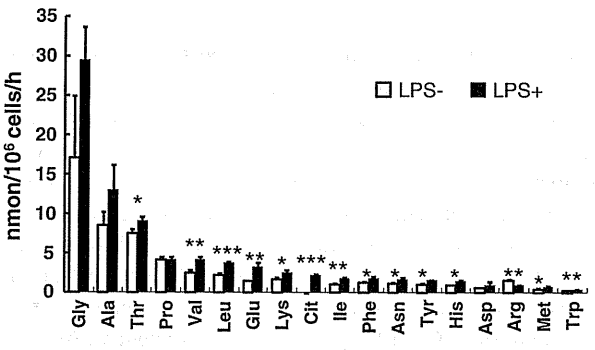

Fig. 4 *Bar graph* showing amino acid production profiles in LPS+ and LPS− cells. Values are means ± standard deviation. *$P < 0.05$, **$P < 0.01$ and ***$P < 0.001$

were small increases in the production of *o*-succinylhomoserine, glyconate and 2-oxoisopentanoate, which showed high fold-changes compared with most amino acids (>1.7-fold) (Table 1). The biological relevance of these metabolites should be confirmed using other "-omics" data and cellular metabolite profiles.

4 Concluding remarks

In this study, we conducted CE-TOFMS-based metabolomics analysis to identify the metabolites secreted by LPS-stimulated macrophage-like RAW264.7 cells. Cellular activation was confirmed by the increased production of NO, citrulline, TNF-α and prostaglandins E_2 and $F_2\alpha$ by the stimulated cells. In addition to large increases in glycine production, the production of lactate was also enhanced, indicating the activation of glycolysis. Increased production of several intermediates in the TCA cycle was also observed. Of oxidative stress-related metabolites, the production of hypoxanthine was particularly high, although the GSSH/GSH ratio was almost unchanged by LPS stimulation. To understand these conflicting results, studies using integrated cellular metabolomics profiles are needed to elucidate how the observed metabolite changes contribute to the subsequent inflammatory events in periodontal disease. Nevertheless, this report provides the first catalog of the various metabolites secreted by activated macrophages, and complements prior reports on the already well-studied pro-inflammatory proteins that are known to be secreted by macrophages.

Acknowledgments This work was supported by research funds from the Yamagata Prefectural Government and the city of Tsuruoka. We thank Shinobu Abe for technical assistance.

Conflicts of interest The authors have no conflicts of interest to declare.

References

Barnes, V. M., Teles, R., Trivedi, H. M., Devizio, W., Xu, T., Mitchell, M. W., et al. (2009). Acceleration of purine degradation by periodontal diseases. *Journal of Dental Research, 88*(9), 851–855.

Bingle, L., Brown, N. J., & Lewis, C. E. (2002). The role of tumour-associated macrophages in tumour progression: Implications for new anticancer therapies. *Journal of Pathology, 196*(3), 254–265.

Carmans, S., Hendriks, J. J., Thewissen, K., Van den Eynden, J., Stinissen, P., Rigo, J. M., et al. (2010). The inhibitory neurotransmitter glycine modulates macrophage activity by activation of neutral amino acid transporters. *Journal of Neuroscience Research, 88*(11), 2420–2430.

Cronstein, B. N., Montesinos, M. C., & Weissmann, G. (1999a). Salicylates and sulfasalazine, but not glucocorticoids, inhibit leukocyte accumulation by an adenosine-dependent mechanism that is independent of inhibition of prostaglandin synthesis and p105 of NFkappaB. *Proceedings of the National Academy of Sciences of the United States of America, 96*(11), 6377–6381.

Cronstein, B. N., Montesinos, M. C., & Weissmann, G. (1999b). Sites of action for future therapy: An adenosine-dependent mechanism by which aspirin retains its antiinflammatory activity in cyclooxygenase-2 and NFkappaB knockout mice. *Osteoarthritis and Cartilage, 7*(4), 361–363.

Ghezzi, P. (2011). Role of glutathione in immunity and inflammation in the lung. *International Journal of General Medicine, 4*, 105–113.

Giannobile, W. V., Beikler, T., Kinney, J. S., Ramseier, C. A., Morelli, T., & Wong, D. T. (2009). Saliva as a diagnostic tool for periodontal disease: Current state and future directions. *Periodontology, 2000*(50), 52–64.

Kand'ar, R., Zakova, P., & Muzakova, V. (2006). Monitoring of antioxidant properties of uric acid in humans for a consideration measuring of levels of allantoin in plasma by liquid chromatography. *Clinica Chimica Acta, 365*(1–2), 249–256.

Kim, J. M., Jeong, D., Kang, H. K., Jung, S. Y., Kang, S. S., & Min, B. M. (2007). Osteoclast precursors display dynamic metabolic shifts toward accelerated glucose metabolism at an early stage of RANKL-stimulated osteoclast differentiation. *Cellular Physiology and Biochemistry, 20*(6), 935–946.

Li, P., Yin, Y. L., Li, D., Woo Kim, S., & Wu, G. (2007). Amino acids and immune function. *British Journal of Nutrition, 98*(02), 237–252.

Meyer, M. S., Joshipura, K., Giovannucci, E., & Michaud, D. S. (2008). A review of the relationship between tooth loss, periodontal disease, and cancer. *Cancer Causes and Control, 19*(9), 895–907.

Nakamura, Y., Kodama, H., Satoh, T., Adachi, K., Watanabe, S., Yokote, Y., et al. (2010). Diurnal changes in salivary amino acid concentrations. *In Vivo, 24*(6), 837–842.

Nakamura, Y., Matsumoto, S., Mochida, T., Nakamura, K., Takehana, K., & Endo, F. (2009). Glycine regulates proliferation and differentiation of salivary-gland-derived progenitor cells. *Cell and Tissue Research, 336*(2), 203–212.

Nareika, A., He, L., Game, B. A., Slate, E. H., Sanders, J. J., London, S. D., et al. (2005). Sodium lactate increases LPS-stimulated MMP and cytokine expression in U937 histiocytes by enhancing AP-1 and NF-kappaB transcriptional activities. *American Journal of Physiology—Endocrinology and Metabolism, 289*(4), E534–E542.

Nishiyama, A., Yokote, Y., & Sakagami, H. (2010). Changes in amino acid metabolism during activation of mouse macrophage-like cell lines. *In Vivo, 24*(6), 857–860.

Noda, M., Nakanishi, H., Nabekura, J., & Akaike, N. (2000). AMPA-kainate subtypes of glutamate receptor in rat cerebral microglia. *The Journal of Neuroscience, 20*(1), 251.

Noguchi, K., & Ishikawa, I. (2007). The roles of cyclooxygenase-2 and prostaglandin E_2 in periodontal disease. *Periodontology, 2000*(43), 85–101.

Paradise, W. A., Vesper, B. J., Goel, A., et al. (2010). Nitric oxide: Perspectives and emerging studies of a well known cytotoxin. *International Journal of Molecular Sciences, 11*, 2715–2745.

Pihlstrom, B. L., Michalowicz, B. S., & Johnson, N. W. (2005). Periodontal diseases. *The Lancet, 366*(9499), 1809–1820.

Ralph, P., & Nakoinz, I. (1977). Antibody-dependent killing of erythrocyte and tumor targets by macrophage-related cell lines: Enhancement by PPD and LPS. *Journal of Immunology, 119*(3), 950–954.

Rausch-Fan, X., Ulm, C., Jensen-Jarolim, E., Schedle, A., Boltz-Nitulescu, G., Rausch, W. D., et al. (2005). Interleukin-1beta-induced prostaglandin E_2 production by human gingival fibroblasts is upregulated by glycine. *Journal of Periodontology, 76*(7), 1182–1188.

Rodriguez-Prados, J. C., Traves, P. G., Cuenca, J., Rico, D., Aragones, J., Martin-Sanz, P., et al. (2010). Substrate fate in activated macrophages: A comparison between innate, classic, and alternative activation. *Journal of Immunology, 185*(1), 605–614.

Roiniotis, J., Dinh, H., Masendycz, P., Turner, A., Elsegood, C. L., Scholz, G. M., et al. (2009). Hypoxia prolongs monocyte/macrophage survival and enhanced glycolysis is associated with their maturation under aerobic conditions. *Journal of Immunology, 182*(12), 7974–7981.

Rose, M. L., Rivera, C. A., Bradford, B. U., Graves, L. M., Cattley, R. C., Schoonhoven, R., et al. (1999). Kupffer cell oxidant production is central to the mechanism of peroxisome proliferators. *Carcinogenesis, 20*(1), 27–33.

Samuvel, D. J., Sundararaj, K. P., Nareika, A., Lopes-Virella, M. F., & Huang, Y. (2009). Lactate boosts TLR4 signaling and NF-kappaB pathway-mediated gene transcription in macrophages via monocarboxylate transporters and MD-2 up-regulation. *Journal of Immunology, 182*(4), 2476–2484.

Soga, T., Baran, R., Suematsu, M., Ueno, Y., Ikeda, S., Sakurakawa, T., et al. (2006). Differential metabolomics reveals ophthalmic acid as an oxidative stress biomarker indicating hepatic glutathione consumption. *Journal of Biological Chemistry, 281*(24), 16768–16776.

Soga, T., Igarashi, K., Ito, C., Mizobuchi, K., Zimmermann, H. P., & Tomita, M. (2009). Metabolomic profiling of anionic metabolites by capillary electrophoresis mass spectrometry. *Analytical Chemistry, 81*(15), 6165–6174.

Soga, T., Ohashi, Y., Ueno, Y., Naraoka, H., Tomita, M., & Nishioka, T. (2003). Quantitative metabolome analysis using capillary electrophoresis mass spectrometry. *Journal of Proteome Research, 2*(5), 488–494.

Stuckey, D., Anthony, D., Lowe, J., Miller, J., Palm, W., Styles, P., et al. (2005). Detection of the inhibitory neurotransmitter GABA in macrophages by magnetic resonance spectroscopy. *Journal of Leukocyte Biology, 78*(2), 393.

Sugimoto, M., Goto, H., Otomo, K., Ito, M., Onuma, H., Suzuki, A., et al. (2010a). Metabolomic profiles and sensory attributes of edamame under various storage duration and temperature conditions. *Journal of Agriculture and Food Chemistry, 58*(14), 8418–8425.

Sugimoto, M., Wong, D. T., Hirayama, A., Soga, T., & Tomita, M. (2010b). Capillary electrophoresis mass spectrometry-based saliva metabolomics identified oral, breast and pancreatic cancer-specific profiles. *Metabolomics, 6*(1), 78–95.

Takahashi, J., Sekine, T., Nishishiro, M., Arai, A., Wakabayashi, H., Kurihara, T., et al. (2008). Inhibition of NO production in LPS-stimulated mouse macrophage-like cells by trihaloacetylazulene derivatives. *Anticancer Research, 28*(1A), 171–178.

Takeda, I., Stretch, C., Barnaby, P., Bhatnager, K., Rankin, K., Fu, H., et al. (2009). Understanding the human salivary metabolome. *NMR in Biomedicine, 22*(6), 577–584.

Tanaka, S., Machino, M., Akita, S., Yokote, Y., & Sakagami, H. (2010). Changes in salivary amino acid composition during aging. *In Vivo, 24*(6), 853–856.

Van Dyke, T. E., & Serhan, C. N. (2003). Resolution of inflammation: A new paradigm for the pathogenesis of periodontal diseases. *Journal of Dental Research, 82*(2), 82–90.

Xu, F. L., You, H. B., Li, X. H., Chen, X. F., Liu, Z. J., & Gong, J. P. (2008). Glycine attenuates endotoxin-induced liver injury by downregulating TLR4 signaling in Kupffer cells. *American Journal of Surgery, 196*(1), 139–148.

Yamashina, S., Ikejima, K., Rusyn, I., & Sato, N. (2007). Glycine as a potent anti-angiogenic nutrient for tumor growth. *Journal of Gastroenterology and Hepatology, 22*(Suppl 1), S62–S64.

Yamazaki, T., Yamazaki, A., Onuki, H., Hibino, Y., Yokote, Y., Sakagami, H., et al. (2007). Effect of saliva, epigallocatechin gallate and hypoxia on Cu-induced oxidation and cytotoxicity. *In Vivo, 21*(4), 603–607.

Ⅲ　メタボロミクス

CE-MSメタボローム測定法

平山　明由 *Akiyoshi Hirayama*（慶應義塾大学先端生命科学研究所）
曽我　朋義 *Tomoyoshi Soga*（慶應義塾大学先端生命科学研究所教授）

Key Words
メタボロミクス
メタボローム
キャピラリー電気泳動-質量分析法（CE-MS）
糖尿病性腎症
バイオマーカー

はじめに

ポストゲノム研究の新しい手法として近年注目を集めているメタボロミクスは，細胞内代謝産物を網羅的に探索することによって生命現象を包括的に理解しようとする方法論である。代謝物は生命システムにおける最終産物であり，その変動は生物の環境応答や適応変化などを最も鋭敏に反映していると考えられている。また，疾病などによって代謝の変動がある場合，血液や尿などに存在する代謝物質の組成や濃度にも変化が起こると考えられるため，各種の疾患バイオマーカーの探索なども精力的に行われている。

メタボローム測定における分析化学的なアプローチとしては，質量分析装置（Mass Spectrometer：MS）を用いたものが主流であるが，特に筆者らはイオン性化合物に対して高分離能を示すキャピラリー電気泳動（Capillary Electrophoresis：CE）とMSをタンデムに接続したCE-MS法を世界に先駆けて開発し，数千種類の代謝物の一斉測定を可能にした[1]。本稿では，CE-MS（図1）を用いたメタボローム解析法の概略とそれを糖尿病性腎症のバイオマーカー探索に適用した例について紹介する。糖尿病性腎症のバイオマーカー探索は名古屋大学医学部，中部ろうさい病院との共同研究の成果である。

図1．キャピラリー電気泳動-飛行時間型質量分析装置（CE-TOFMS）